BEST AVAILABLE IMAGES

Defective images within this document are accurate representations of the original documents submitted by the applicant.

Defects in the images may include (but are not limited to):

- BLACK BORDERS
- TEXT CUT OFF AT TOP, BOTTOM OR SIDES
- FADED TEXT
- ILLEGIBLE TEXT
- SKEWED/SLANTED IMAGES
- COLORED PHOTOS
- BLACK OR VERY BLACK AND WHITE DARK PHOTOS
- GRAY SCALE DOCUMENTS

IMAGES ARE BEST AVAILABLE COPY.

As rescanning documents *will not* correct images, please do not report the images to the Image Problem Mailbox.

13. A method for augmenting at least one physical catalyst in a chemical reaction comprising the steps of:

a) determining at least one frequency selected from the group of frequencies consisting of (a) at least one frequency of a duplicated electromagnetic pattern of said at least one physical catalyst, (b) at least one harmonic frequency of an electromagnetic pattern of said at least one physical catalyst and (c) at least one frequency which copies at least one mechanism of action of said at least one physical catalyst ; and

b) exposing said chemical reaction system to said at least frequency from said group of frequencies, said exposing being sufficient to augment said at least one physical catalyst.

The pending independent claims broadly recite:

1. **Determining;**
2. **Duplicating;** and
3. **Exposing.**

Determining an electromagnetic spectral pattern (claim 1) or determining the claimed at least one frequency (claim 13) can both utilize the spectroscopy techniques disclosed in the present specification at pages 11-16. Specifically, pages 11-16 of the present specification describe in detail various methods of spectroscopy well known to those of ordinary skill in the art. These methods include absorption and emission spectra as well as, for example, microwave spectroscopy, radio spectroscopy and Raman spectroscopy. While some of the disclosed spectroscopy techniques are distinct from absorption or emission spectroscopy, all of these techniques are well known. However, the claimed **determining of at least a portion of the spectral pattern of a physical catalyst is not disclosed or suggested by the prior art.** The Action alleges that some "special" pattern is used. This simply is not the case. The spectral patterns utilized are ordinary spectroscopy patterns known to the art.

The claimed **duplicating** (e.g., claim 1) of at least one **determined** frequency of a physical catalyst is required in order to achieve the claimed **augmenting** of a physical catalyst (e.g., these claims recite the presence of a physical catalyst and at least one frequency of a physical catalyst which are determined by the discussed spectroscopy techniques).

Further, the claimed **exposing** of the reaction system to at least one frequency of the spectral pattern is one of the important steps in achieving the claimed **augmenting.**

These claimed steps are straightforward and well supported by the present specification. Applicants recognize that these concepts are new to the Examiner because no one ever before understood these important aspects of catalysis. The Action refers to "the well established field of kinetics" and recognizes that the field of kinetics has not resolved how catalysis occurs on the atomic and molecular levels. Applicants respectfully suggest that the present invention fills in some of those holes. Further, applicants hereby attach two Articles from Science ,Volume 302, pp 70-71 and 98-100 which seem to support some of applicants' assertions. These related articles state, for example, at page 98, the end of the first full paragraph of the bottom article:

> "Despite intense effort, there is still no atomic-scale picture of the dynamics of this important gas-surface reaction."

Further, at page 71, the bottom of the top middle section, the following appears:

> "The results provide unambiguous evidence that the theoretical assumptions underlying the statistical model are incorrect, thus paving the way for mode-selective catalysis."

The reference to the above-mentioned "statistical model" is referring to the well established field of kinetics. The articles support Applicants' contentions that catalysis is much more than merely kinetics and involves frequency specific interactions, thus suggesting the accuracy of applicants' contentions and claims.

Moreover, the reference in the Action to "photochemistry" is misplaced. Applicants were well aware of photochemistry techniques at the time of filing this application (e.g., see the present specification at page 4 lines 1-12). However, the field of photochemistry by itself does not make any reference to the importance of the claimed features of the pending claims.

Further, the Action at the top of page 4 questions the efficacy of the Examples. Applicants direct the attention of the Examiner to Example 5 at page 27, line 15 – page 28, line 6. This Example discusses the augmenting of a physical catalyst. For example, page 27, lines

27-30 discuss augmenting physical platinum catalyst with the spectral catalyst platinum emitted from hollow cathode platinum lamps (Fisher Scientific). These lamps emitted the spectral pattern of platinum which is the known catalyst for the reaction. Thus, the reaction system comprising hydrogen and oxygen gasses and physical platinum catalyst was exposed to the spectral pattern of platinum. This exposure resulted in "a mean increase in reaction rate of approximately 60%" (page 28, lines 3-6).

Claims 1-4 and 7-15 stand rejected under Section 103(a). This rejection is also respectfully traversed.

The combined references are combined from hindsight alone. The first set of four references beginning with Gdowski et al, relate to the field of surface chemistry. The second set of two references to Volman are related to ordinary photochemistry. The final reference to Sansonetti comprises calibration data for the Hubble Space Telescope. There simply is no motivation to combine these references absent Applicants' own teachings. Specifically, these set of references alone or in combination do not disclose or suggest the claimed **determining**, **duplicating** and **exposing** to achieve the claimed **augmenting of a physical catalyst**. The prior art simply does not recognize the importance of these claimed features

Applicant respectfully requests a favorable action on the merits of the Application.

Respectfully submitted,

Mark G. Mortenson
Reg. No. 31,182

The Law Offices of Mark G. Mortenson
Post Office Box 310
North East, MD 21901-0310
Telephone: 410-287-8795
Telefax: 410-287-5046

adsorbed copper phthalocyanine (CuPc) molecules (*6*). The atomic corrugation of the (110) surface ensures that the Au atoms are aligned in straight chains and that a single CuPc molecule snaps into the position corresponding to its most favorable bonding site.

The authors used a STM tip to form two lines of Au atoms with a separation of three to six lattice constants. They then positioned a CuPc molecule between the two lines of Au atoms. The tightest binding and best electronic overlap occurred when the CuPc was placed between Au lines with a spacing of five lattice constants (see the figure). The CuPc molecule has a symmetric cross shape. It fits snuggly into the five–lattice constant gap between the two Au lines, with one of the axes of the CuPc bridging the Au-Au junction. This final assembly is a perfectly ordered metal-molecule-metal junction of known atomic structure.

By imaging the spatial distribution of the electronic density of states in the junction, the authors were able to determine how the molecular orbitals spanned the metal-molecule-metal junction. In addition, they used scanning tunneling spectroscopy to determine the electronic structure of the Au chains as the chain lengths were increased from one to six atoms. Upon bonding to CuPc, the electronic state of the first Au atom in each of the two chains is altered, changing its interactions with the rest of the Au chain. The bonding of the CuPc to the first Au atom on each end of the two chains is so strong that these Au atoms become part of an "extended" CuPc molecule. By systematically appending individual atoms to the chains, Nazin *et al.* could tune the energies of the chain states to those of the extended molecule.

The formation of the "extended" molecule changes the degree of coupling between the molecular and metal states and thus the conductivity of the junction. This coupling between the molecule and metal states is critical for understanding metal-molecule-metal junctions in the nascent field of molecular electronics.

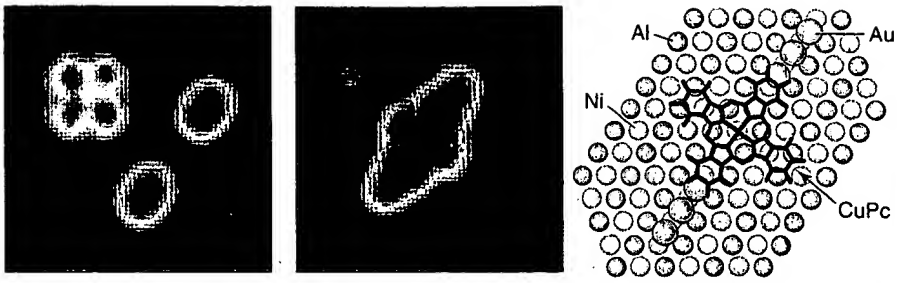

Assembly kit for metal-molecule junctions. (Left) The two bright ovals in this 49 Å by 49 Å STM image each consists of a chain of three Au atoms, which have been assembled atom by atom with an STM tip on NiAl(110). The end atoms of the chains are separated by five lattice constants. **(Center)** A CuPc molecule is moved toward the chains and snaps into position between the ends of the Au chains. The STM contrast of Au atoms bound to the CuPc differs from that of the more distant Au atoms. **(Right)** Ball-and-stick diagram of CuPc bound to the Au chains. The spacing of the chain ends allows the molecule to form strong bonds with the Au atoms at the end of the chains.

References and Notes

1. Y. Hirose, C. I. Wu, V. Aristov, P. Soukiassian, A. Kahn, *Appl. Surf. Sci.* **113-114**, 291 (1997).
2. In ohmic contacts, the current across the contact has a strict linear dependence upon the voltage across the contact. When there is a Schottky barrier, the current across the contact will have a nonlinear dependence on the applied voltage.
3. G. V. Nazin, X. H. Qiu, W. Ho, *Science* **302**, 77 (2003); published online 4 September 2003 (10.1126/science.1088971).
4. J. Reichert, R. Ochs, D. Beckmann, H. B. Weber, M. Mayor, Hy. Lohneysen, *Phys. Rev. Lett.* **88**, 176804-1 (2002).
5. See also http://rugth30.phys.rug.nl/msc_thinfilmphys/single.htm.
6. A CuPc molecule consists of a Cu atom at the center of a fourfold symmetric cross of aromatic rings.

CHEMISTRY

Toward Vibrational Mode Control in Catalysis

A. C. Luntz

When an atom and a molecule encounter each other in the gas phase, vibrational excitation of the molecule along the reaction coordinate generally increases the reactivity substantially. When the reacting molecule has several different chemical bonds, vibrational excitation of a specific bond can be used to control the reaction outcome (*1*). On page 98 of this issue, Beck *et al.* (*2*) pave the way for extending such bond-selective chemistry from gas-phase to surface-catalyzed reactions.

There are two principal requirements for bond-selective chemistry: a means to excite a specific bond (or local mode), and localization of the energy in this bond until reaction occurs. The first condition is usually met by laser excitation of a local mode. The second requires that the internal vibrational redistribution rate is slow relative to the reaction rate.

Both conditions can often be met for fast direct gas-phase reactions (*1*), but it has been unclear whether the second condition can be satisfied for the activated dissociation of molecules at a gas-surface interface. These reactions are the rate-limiting steps in many technologically (and economically) important heterogeneous catalytic processes. Beck *et al.* (*2*) unequivocally answer this question in the affirmative by measuring the activated dissociation of methane (CH_4) prepared in different vibrational modes on a Ni(100) surface.

Surface scientists have tried for decades to understand the activated dissociation of CH_4 on transition metal surfaces. The reaction has attracted so much interest because CH_4 dissociative adsorption on a supported Ni catalyst limits the rate of the industrially important steam reforming process [which converts natural gas to a mixture of CO and H_2 ("syn gas")]. A detailed microscopic understanding of this step may lead to a better catalyst. However, the activated dissociation of CH_4 on a metal surface is such a complex multidimensional dynamical process that the microscopic description of this process remains controversial (*3*).

There are two main competing views of this process. One is that activated dissociation is a direct dynamical process, much like that in a direct gas-phase bimolecular reaction. The challenge then is to reduce the dimensionality of the dynamical treatment to the essential features (*3*). The other view is that activated dissociation is a purely statistical process (*4*). This is also a well-known mechanism for gas-phase reactions, but only when long-lived collision complexes are formed so that the energy is randomized in the collision complex before reaction. The statistical picture greatly simplifies the description of the reaction dynamics. Both experiment and theory provide evidence that the CH_4-surface collision complex is short-lived (about 10^{-13} s),

The author is affiliated with the Department of Physics, University of Southern Denmark, 5230 Odense M, Denmark. E-mail: acluntz@pacbell.net

and the justification for such a mechanism is therefore based on the high dimensionality of the CH_4-surface collision complex. In this case, it is suggested that the high density of states makes the internal vibrational redistribution fast compared to the short collision lifetime.

Numerous molecular beam studies of activated CH_4 dissociation on transition metal surfaces have shown a strong and interrelated dependence of the dissociation probability on initial CH_4 translational energy, CH_4 vibrational temperature, and surface temperature [e.g., (*5*)]. These experimental data can be fit both to dynamical (*6*) and statistical (*4*) models. Hence, "fits" to a model are not by themselves sufficient to test the underlying theoretical assumptions.

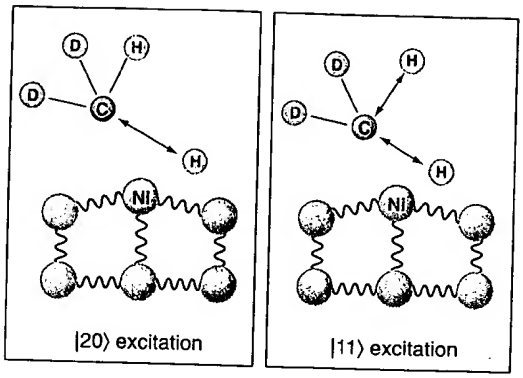

Excitation with a difference. Schematic representation of two different local vibrational modes, $|20\rangle$ and $|11\rangle$, of CH_2D_2 near the transition state for dissociation on a Ni(100) surface. The Ni surface atoms are connected by springs to emphasize that the reaction also involves a substantial lattice distortion at the transition state and energy transfer with the lattice.

However, the two opposing views of activated dissociation predict an entirely different vibrational mode–specific behavior. The statistical mechanism depends only on the total energy of the collision complex and does not allow any mode-specific behavior. In contrast, the dynamical mechanism does allow mode-specific behavior if the different vibrational modes have different projections onto the reaction coordinate, especially in the region of the barrier. Ab initio electron structure calculations for CH_4 dissociation on a nickel surface show that the reaction coordinate at the transition state is dominated by extension of a single C-H bond, which is broken during the course of the dissociative adsorption (*7*).

Beck *et al.* compare the dissociation probabilities for two different vibrational states of CH_2D_2 at nearly the same energy: $|20\rangle$ has two quanta of excitation localized in a single C-H bond, whereas $|11\rangle$ has the two quanta of excitation localized in two different C-H bonds. For the optimal orientation of the molecule's collision with the surface, these modes have different projections onto the reaction coordinate in the region of the transition state (see the figure), and thus different reactivities. The results provide unambiguous evidence that the theoretical assumptions underlying the statistical model are incorrect, thus paving the way for mode-selective catalysis.

The application of laser mode excitation to activated dissociation at surfaces, pioneered by Beck *et al.* and others (*8, 9*), is still in its infancy. Further studies of different modes in systems such as CH_4/Ni(100) should allow far more sophisticated dynamical questions to be probed in detail. For example, what are the roles of bending and stretching vibrations in the activation? How nonstatistical are the dynamics? Are the complex dynamics best described as a multidimensional dynamical problem or as a dynamically constrained statistical process (*10*)?

The results reported by Beck *et al.* should stimulate ab initio theorists to tackle this challenging problem, much as has been done for the similar but simpler problem of H_2 dissociation on metal surfaces (*11*). We should then be able to assess properly the viability of vibrational state control in heterogeneous catalysis.

References

1. F. F. Crim, *Acc. Chem. Res.* **32**, 877 (1999).
2. R. D. Beck *et al.*, *Science* **302**, 98 (2003).
3. A. C. Luntz, J. Harris, *Surf. Sci.* **258**, 397 (1991).
4. V. A. Ukraintsev, I. Harrison, *J. Chem. Phys.* **101**, 1564 (1994).
5. P. M. Holmblad, J. Wambach, I. Chorkendorff, *J. Chem. Phys.* **102**, 8255 (1995).
6. A. C. Luntz, *J. Chem. Phys.* **102**, 8264 (1995).
7. P. Kratzer, B. Hammer, J. K. Nørskov, *J. Chem. Phys.* **105**, 5595 (1996).
8. L. B. F. Juurlink *et al.*, *Phys. Rev. Lett.* **83**, 868 (1999).
9. J. Higgins, A. Conjusteau, G. Scoles, S. L. Bernasek, *J. Chem. Phys.* **114**, 5277 (2001).
10. H. Mortensen, L. Diekhoner, A. Baurichter, A. C. Luntz, *J. Chem. Phys.* **116**, 5781 (2002).
11. G. J. Kroes, *Prog. Surf. Sci.* **60**, 1 (1999).

PLANT BIOLOGY

Hormones and the Green Revolution

Francesco Salamini

In his famous 1840 manifesto, Justus Liebig advocated a more rational approach to agronomic research. He proposed integrating physiological and chemical principles to improve the yield of crop plants. However, it was not until after World War II that agronomists, searching for better herbicides and insecticides (*1*), took a rational approach to boosting crop yields. The creation of genetically improved crop varieties, in particular dwarf cultivars of wheat and rice (see the figure), resulted in the doubling of food grain production within a few decades, a success dubbed the green revolution (*2*). The short stature and sturdy stalks of the dwarf varieties of wheat and rice rendered them resistant to flattening by wind, rain, or high densities (lodging) and more effective in converting fertilizer input into higher yields. For example, short semi-dwarf wheat varieties exhibit a 100% greater yield than earlier, taller cultivars (*3*). The genes responsible for the rice and wheat green revolution dwarf varieties have been identified. They encode proteins that either regulate synthesis of the plant growth hormone gibberellin or modulate its signaling pathway. On page 81 of this issue, Multani *et al.* (*4*) identify a new mechanism controlling plant height in maize and sorghum dwarf mutants of agronomic importance. They show that the mutant gene in the brachytic2 (*br2*) maize mutant and the dwarf3 (*dw3*) sorghum mutant encodes a protein responsible for the transport of auxin, the first plant growth hormone to be discovered.

Enhanced online at www.sciencemag.org/cgi/content/full/302/5642/71

A rational approach to improving crop varieties depends on a better understanding of plant biology. Of the tens of thousands of genes in plant genomes, one needs to know not only which genes control complex traits like size or yield but also how these genes limit successful plant-breeding programs. There are several strategies for elucidating how genes affect the phenotypes of plants. One approach is to analyze quantitative trait loci (QTL), which reveal allelic variations that can be exploited in plant breeding (*5*). Another approach is to screen plant genomes for a genetic signature, which indicates strong selection for a specific set of genes that generates modi-

The author is at the Max Planck Institute of Breeding Research, 50829 Köln, Germany. E-mail: salamini@mpiz-koeln.mpg.de

croscope. Longer modulated waveguides with shorter modulation periods should significantly enhance the signal for several reasons. First, $m = 1$ QPM should become possible by using shorter periods. Second, the 2.5-cm modulated waveguide length corresponds to only 0.3 absorption depths in Ne at 284 eV. Previous theoretical studies have indicated that 5 to 10 absorption depths are ideal for generating a maximum signal (*32*). Furthermore, because the highest HHG photon energy scales linearly with laser intensity, using very reasonable laser parameters (i.e., pulsewidth ~10 fs, intensities $\sim 5 \times 10^{15}$ W cm^{-2}) and waveguides with 0.1 mm periodicity, we should be able to generate high-order quasi–phase-matched light at photon energies approaching 1 keV.

References and Notes

1. R. Schoenlein *et al.*, *Science* **287**, 2237 (2000).
2. D. Attwood, *Phys. Today* **45**, 24 (August, 1992).
3. C. Jacobsen, *Trends Cell Biol.* **9**, 44 (1999).
4. G. Schneider *et al.*, *Surf. Rev. Lett.* **9**, 177 (February, 2002).
5. A. McPherson *et al.*, *JOSA B* **4**, 595 (1987).
6. M. Ferray *et al.*, *J. Phys. B* **21**, L31 (1987).
7. J. J. Macklin, J. D. Kmetec, C. L. Gordon, III, *Phys. Rev. Lett.* **70**, 766 (1993).
8. R. Haight, P. F. Seidler, *Appl. Phys. Lett.* **65**, 517 (1994).
9. D. Descamps *et al.*, *Opt. Lett.* **25**, 135 (2000).
10. M. Bauer *et al.*, *Phys. Rev. Lett.* **8702**, 5501 (2001).
11. L. Nugent-Glandorf, M. Scheer, D. Samuels, V. Bierbaum, S. Leone, *J. Chem. Phys.* **117**, 6108 (2002).
12. R. A. Bartels *et al.*, *Science* **297**, 376 (2002).
13. A. Rundquist *et al.*, *Science* **280**, 1412 (1998).
14. A. Paul *et al.*, *Nature* **421**, 51 (2003).
15. I. P. Christov, H. C. Kapteyn, M. M. Murnane, *Optics Express* **7**, 362 (2000).
16. Z. H. Chang, A. Rundquist, H. W. Wang, M. M. Murnane, H. C. Kapteyn, *Phys. Rev. Lett.* **79**, 2967 (1997).
17. C. Spielmann *et al.*, *Science* **278**, 661 (1997).
18. S. Backus, C. G. I. Durfee, G. A. Mourou, H. C. Kapteyn, M. M. Murnane, *Opt. Lett.* **22**, 1256 (1997).
19. The harmonic emission emerging from the waveguide passes through Zr or Ag filters (0.4 μm) to block the fundamental light, and the harmonics are then spectrally dispersed onto an Andor CCD camera with a Hettrick EUV spectrometer. The energy calibration of the spectrometer was verified by recording the positions of the Si, B, and C absorption edges, at 99.9 eV, 188.35 eV, and 284 eV, respectively.
20. C. G. Wahlström *et al.*, *Phys. Rev. A* **48**, 4709 (1993).
21. K. C. Kulander, K. J. Schafer, J. L. Krause, in *Super-Intense Laser-Atom Physics*, B. Piraux, A. L'Huillier, K. Rzazewski, Eds. (Plenum, New York, 1993), vol. 316, pp. 95–110.
22. M. V. Ammosov, N. B. Delone, V. P. Krainov, *Soviet Physics JETP* **64**, 1191 (1986).
23. V. P. Krainov, *JOSA B* **14**, 425 (1997).
24. I. P. Christov, M. M. Murnane, H. C. Kapteyn, *Phys. Rev. Lett.* **78**, 1251 (1997).
25. I. P. Christov, M. M. Murnane, H. C. Kapteyn, *Phys. Rev. A* **57**, R2285 (1998).
26. A. Scrinzi, M. Geissler, T. Brabec, *Phys. Rev. Lett.* **83**, 706 (1999).
27. Z. Chang *et al.*, *Phys. Rev. A* **58**, R30 (1998).
28. H. J. Shin *et al.*, *Phys. Rev. A* **63**, 053407 (2001).
29. M. Schnürer *et al.*, *Phys. Rev. Lett.* **83**, 722 (1999).
30. J. Zhou, J. Peatross, M. M. Murnane, H. C. Kapteyn, I. P. Christov, *Phys. Rev. Lett.* **76**, 752 (1996).
31. M. M. Fejer, G. A. Magel, D. H. Jundt, R. L. Byer, *IEEE J. Quantum Electron.* **28**, 2631 (1992).
32. E. Constant *et al.*, *Phys. Rev. Lett.* **82**, 1668 (1999).

33. This work was supported by the National Science Foundation and the Department of Energy and made use of facilities funded by the W. M. Keck Foundation.

1 July 2003; accepted 3 September 2003

Vibrational Mode–Specific Reaction of Methane on a Nickel Surface

Rainer D. Beck,* Plinio Maroni, Dimitrios C. Papageorgopoulos, Tung T. Dang, Mathieu P. Schmid, Thomas R. Rizzo

The dissociation of methane on a nickel catalyst is a key step in steam reforming of natural gas for hydrogen production. Despite substantial effort in both experiment and theory, there is still no atomic-scale description of this important gas-surface reaction. We report quantum state–resolved studies, using pulsed laser and molecular beam techniques, of vibrationally excited methane reacting on the nickel (100) surface. For doubly deuterated methane (CD_2H_2), we observed that the reaction probability with two quanta of excitation in one C-H bond was greater (by as much as a factor of 5) than with one quantum in each of two C-H bonds. These results clearly exclude the possibility of statistical models correctly describing the mechanism of this process and attest to the importance of full-dimensional calculations of the reaction dynamics.

The reaction of methane on a nickel catalyst to form surface-bound methyl and hydrogen is the rate-limiting step in steam reforming, which is the principal process for industrial hydrogen production as well as the starting point for the large-scale synthesis of many important chemicals such as ammonia, methanol, and higher hydrocarbons (*1*). Because of its importance, the dissociation of methane on nickel has been considered a prototype for chemical bond formation between a polyatomic molecule and a solid surface, with many experimental and theoretical studies directed at elucidating its mechanism (*2–14*). In view of the enormous economic importance of this process (*15*), it would be desirable to have a reliable theoretical description that could guide the development of improved catalysts (*2, 3*). Despite intense effort, there is still no atomic-scale picture of the dynamics of this important gas-surface reaction.

Molecular beam experiments (*4–6*) have firmly established that methane chemisorption is a direct process that can be activated with about equal efficiency by both incident kinetic energy normal to the surface and thermal vibrational energy of the incident methane. State-resolved reactivity measurements that used laser excitation of the asymmetric stretch fundamental vibration (ν_3) (*7*) and first overtone ($2\nu_3$) (*8*) of CH_4 incident on Ni(100) have confirmed the notion that vibrational energy is similar to translational excitation in its efficiency in promoting this reaction. Theoretical treatments of methane chemisorption have included wave packet simulations with up to nine vibrational degrees of freedom (*9*), reduced-dimensionality dynamical models with only a single C-H stretch vibration (*10–12*), and a greatly simplified statistical model (*13*). Despite having diametrically opposed presuppositions, both dynamical and statistical approaches claim to reproduce existing experimental data (*10, 16*), although they make different predictions about the role of methane vibrational excitation in promoting the reaction. Some dynamical calculations suggest that the reactivity of vibrationally excited methane on nickel should depend on the precise nature of the vibrational mode (*9, 17*), whereas statistical models predict the complete absence of such effects (*16*). Although the reverse process—the associative desorption of methane from transition metal surfaces—seems to deviate somewhat from a purely statistical model (*18, 19*), the experimental results reported thus far do not exclude either approach, because there is no reported evidence for mode specificity in the surface reaction of methane.

In contrast, mode-specific reactivity of methane in the gas phase has been observed. Yoon *et al.* (*20*) have found that when methane is excited to the symmetric stretch-bend combination $\nu_1 + \nu_4$, it is more reactive with atomic chlorine (by a factor of 1.9) than when it is promoted to the nearly isoenergetic antisymmetric combination $\nu_3 + \nu_4$. In a similar study, Kim *et al.* (*21*) observed that the product state distribution for the reaction of CD_2H_2 with chlorine depends on the initially

Laboratoire Chimie Physique Moléculaire, Ecole Polytechnique Fédérale de Lausanne (EPFL), CH-1015 Lausanne, Switzerland.

*To whom correspondence should be addressed. E-mail: rainer.beck@epfl.ch

prepared reactant vibrational state. Two states with similar energy but different C-H bond stretching amplitudes produce a CD_2H methyl fragment in completely different vibrational states. Both studies show that vibrational energy put into specific modes of methane is not redistributed internally by the reactive encounter, but instead contributes in a mode-specific way to promoting the chemical reaction. It remains unknown whether similar nonstatistical dynamics would occur in the encounter of a gas-phase molecule with a solid surface.

To test for vibrational mode–specific behavior in gas-surface reactions, we performed quantum state–resolved measurements in a molecular beam surface science apparatus, using pulsed laser preparation of vibrationally excited methane molecules incident on a Ni(100) single-crystal surface (*22*). Figure 1 shows a schematic illustration of our experiment. After a deposition time adjusted to produce a surface coverage of about 5% of a monolayer (ML), the products of the dissociative chemisorption of methane were detected as surface-bound carbon by Auger electron spectroscopy. We quantify the amount of deposited carbon by recording C and Ni Auger spectra in a line scan across the surface and calibrate it by comparison with the C/Ni Auger ratio for a known 0.5-ML saturation coverage obtained by extended exposure to a high-energy beam of methane. We use the doubly deuterated isotopomer of methane (CD_2H_2) rather than CH_4 for these experiments because of its spectroscopic properties (*23*). In CD_2H_2, combinations of the two infrared (IR) active C-H stretch fundamentals (ν_1 and ν_6) form nearly isoenergetic states with comparable absorption strength but different nuclear motion, labeled $|20\rangle$ and $|11\rangle$ in local mode notation (*24*).

CD_2H_2 in the molecular beam was excited into either the $|20\rangle$ or the $|11\rangle$ C-H stretch local mode state (*25*). A comparison of the surface carbon Auger signals for incident CD_2H_2 excited to these two states is shown in Fig. 2. To obtain these data, we directed a molecular beam containing 20% CD_2H_2 in H_2 at normal incidence for 15 min at two different positions on the initially clean Ni(100) surface. For the first deposition (left-hand peak), the $|20\rangle$ state of CD_2H_2 with one unit of angular momentum ($J = 1$) was excited by 120-mJ pulses from an IR laser tuned to the $\Delta J = 0$ transition at 5879.8 cm^{-1}, and for the second deposition (right-hand peak), the $J = 1$ level of the $|11\rangle$ state was prepared using the same IR pulse energy to excite the corresponding transition at 6000.2 cm^{-1}. We used cavity ring down spectroscopy (CRDS) (*26*) in a separate free-jet expansion to ensure that the excitation laser remained resonant with the selected transition throughout the deposition. CRDS was also used to determine an upper limit for the rotational temperature of 9 K for the CD_2H_2 in the beam and to measure the absolute transition strength. Although the transition we used to prepare the $|20\rangle$ level is weaker than that used to excite the $|11\rangle$ level by a factor of 1.5 ± 0.1, the former leads to a carbon signal at least three times as large, indicating clear mode-specific behavior. Control experiments such as reversing the order and surface location of the deposition did not change the result. Experiments under identical beam conditions but without laser excitation showed no detectable carbon signal above the background. To measure the reactivity of the unexcited methane beam, we increased the flux by a factor of 80 and used a deposition time of up to 110 min. Our laser-off measurements represent only an upper limit for the reactivity of CD_2H_2 in the vibrational ground state because of a small fraction of thermally excited CD_2H_2 in the molecular beam. Both laser-on and laser-off measurements were made for a series of incident kinetic energies. At each energy, the experiment was repeated up to 10 times. Figure 3 shows the state-resolved sticking coefficients for CD_2H_2 determined from these measurements.

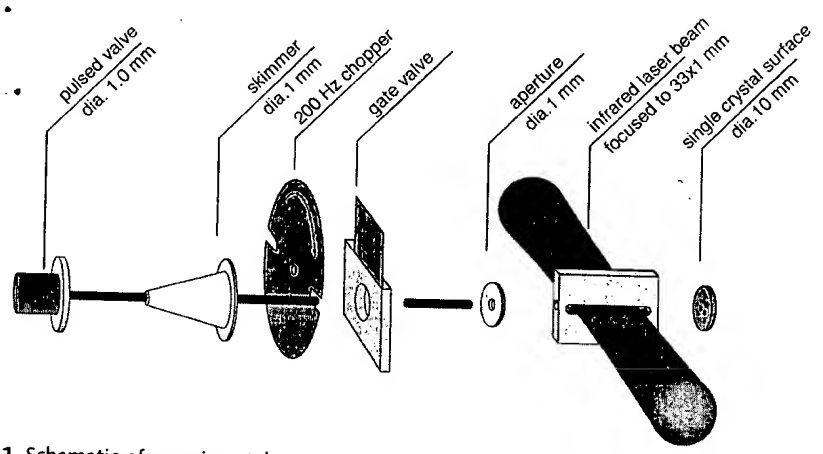

Fig. 1. Schematic of experimental setup. We prepared methane under collision-free conditions by expanding it in a mixture with hydrogen gas through a solenoid-actuated pulsed valve operating at 20 Hz. The resulting supersonic jet expansion accelerates the methane molecules to a kinetic energy controlled by the methane/H_2 seed ratio and the valve temperature, as determined by time-of-flight measurements. The free-jet expansion was skimmed, and the resulting molecular beam was sliced into 30-μs pulses by a chopper wheel. Before the molecular beam impinged on the sample surface (Ni single crystal 10 mm in diameter, cut within 0.1° of the 100 plane), it was irradiated by pulsed, tunable IR light to prepare a fraction (1 to 2%) in a specific ro-vibrationally excited quantum state. Sticking coefficients averaged over all vibrational states of methane populated in the beam were obtained from the ratio of the carbon coverage to the incident methane dose. Sticking coefficients for the state-selected methane molecules were calculated from the difference obtained with the laser on and off, because contributions from the small amount of thermally excited vibrational states in the beam drop out of this difference (*7*).

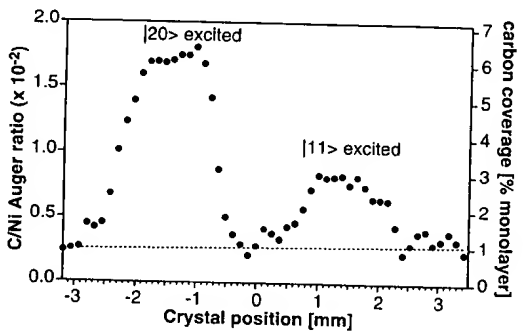

Fig. 2. Surface carbon Auger signal for identical doses of CD_2H_2 excited to the $|20\rangle$ and $|11\rangle$ vibrational states incident on a Ni(100) surface at kinetic energy of 41 kJ/mol. The dotted line indicates the background level of carbon accumulated during the deposition and analysis time.

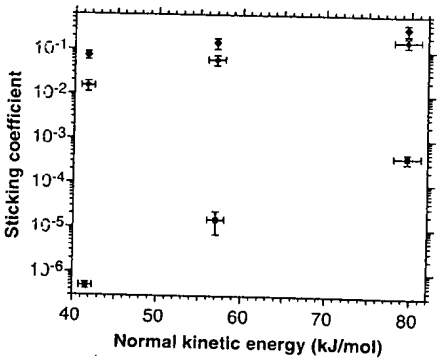

Fig. 3. State-resolved sticking coefficients for CD_2H_2 in (from top to bottom) the $|20\rangle$ (◆), $|11\rangle$ (●), and ground (■) vibrational states on Ni(100) as a function of incident kinetic energy normal to the surface. The surface temperature is 473 K.

At 41 kJ/mol, the lowest incident kinetic energy investigated so far, we find that CD_2H_2 is 5.4 times as reactive when promoted to the $|20\rangle$ state relative to the $|11\rangle$ state. The reactivity for both states is enhanced by several orders of magnitude with respect to incident molecules in the ground vibrational state with the same kinetic energy. The relative reactivity of the $|20\rangle$ and $|11\rangle$ states decreases with increasing kinetic energy, reaching a factor of 2 at a kinetic energy of 80 kJ/mol. At still higher kinetic energy we observe a continuation of this trend, although an accurate determination of the absolute reactivity becomes increasingly difficult as a result of the higher reactivity of the ground-state molecules. This decrease in mode specificity is likely due to the increase of the total amount of available energy relative to the reaction barrier. As the reaction probability approaches its asymptotic value, the difference between the two vibrational modes is expected to decrease. On the other hand, the mode selectivity should be even larger at lower kinetic energy.

The increased reactivity of the $|20\rangle$ level relative to $|11\rangle$ can be rationalized in terms of their different vibrational amplitudes: The former contains two quanta of stretch vibration in a single C-H bond, whereas the latter contains one quantum in each of two C-H bonds. In the gas-phase reaction of CD_2H_2 with chlorine, the product state distributions observed by Kim *et al.* (*21*) confirm this local mode description by demonstrating that one of the two bonds acts as a spectator during the reaction. The same description also rationalizes our observation of higher reactivity of the $|20\rangle$ state in terms of the larger vibrational amplitude along the C-H bond relative to $|11\rangle$. This difference in reactivity implies that the C-H bond stretch has a substantial projection on the reaction coordinate, in agreement with ab initio calculations of the transition-state structure (*27*).

Our observation of vibrational mode–specific gas-surface reactivity has important implications for theoretical treatments of this process. Mode-specific reactivity is inconsistent with the existence of a transient physisorbed complex, as has been suggested in the statistical model proposed by Harrison (*13*). His model assumes complete intramolecular redistribution of the initial vibrational energy in methane as it transiently resides in a local "hot spot" and weakly interacts with a limited number of surface atoms, and it determines rates for desorption and dissociation according to microcanonical rate theory. As a result, it predicts a reactivity that scales only with the total available energy independent of vibrational mode, which is inconsistent with our experimental results. In contrast to the assumptions of this (or any) statistical model, our observation that CH_2D_2 retains a clear memory of the initially prepared quantum state indicates that its interaction with the metal surface does not induce extensive intramolecular energy redistribution before the reaction occurs.

In addition to excluding statistical assumptions, the observation of mode specificity in the reaction probability provides guidance for dynamical models. It suggests that a realistic description of the chemical dynamics will need to go beyond low dimensionality. Calculations including all nine vibrational degrees of freedom of the incident molecule are now starting to become feasible (*9*, *28*), and our experimental results provide stringent tests for such calculations as well as reassurance that efforts in this direction are warranted.

References and Notes

1. P. L. Spath, M. K. Mann, National Renewable Energy Laboratory Technical Report NREL/TP-570-27637 (2001).
2. H. J. Larsen, I. Chorkendorff, *Surf. Sci. Rep.* **35**, 163 (1999).
3. F. Besenbacher *et al.*, *Science* **279**, 1913 (1998).
4. C. T. Rettner, H. E. Pfnür, D. J. Auerbach, *Phys. Rev. Lett.* **54**, 2716 (1985).
5. M. B. Lee, Q. Y. Yang, S. T. Ceyer, *J. Chem. Phys.* **87**, 2724 (1987).
6. P. M. Holmblad, J. Wambach, I. Chorkendorff, *J. Chem. Phys.* **102**, 6255 (1995).
7. L. B. F. Juurlink, P. R. McCabe, R. R. Smith, C. L. DiCologero, A. L. Utz, *Phys. Rev. Lett.* **83**, 868 (1999).
8. M. P. Schmid, P. Maroni, R. D. Beck, T. R. Rizzo, *J. Chem. Phys.* **117**, 8603 (2002).
9. R. Milot, A. P. J. Jansen, *Phys. Rev. B* **61**, 15657 (2000).
10. A. C. Luntz, *J. Chem. Phys.* **102**, 8264 (1995).
11. M.-N. Carré, B. Jackson, *J. Chem. Phys.* **108**, 3722 (1998).
12. Y. Xiang, J. Z. H. Zhang, *J. Chem. Phys.* **118**, 8954 (2003).
13. V. A. Ukraintsev, I. Harrison, *J. Chem. Phys.* **101**, 1564 (1994).
14. J. Higgins, A. Conjusteau, G. Scoles, S. L. Bernasek, *J. Chem. Phys.* **114**, 5277 (2001).
15. I. Maxwell, *Stud. Surf. Sci. Catal.* **101**, 1 (1996).
16. A. Bukoski, I. Harrison, *J. Chem. Phys.* **118**, 9762 (2003).
17. L. Halonen, S. L. Bernasek, D. J. Nesbitt, *J. Chem. Phys.* **115**, 5611 (2001).
18. K. Watanabe, M. C. Lin, Y. A. Gruzdkov, Y. Matsumoto, *J. Chem. Phys.* **104**, 5974 (1996).
19. H. Mortensen, L. Diekhöner, A. Baurichter, A. C. Luntz, *J. Chem. Phys.* **116**, 5781 (2002).
20. S. Yoon, S. Henton, A. N. Zivkovic, F. F. Crim, *J. Chem. Phys.* **116**, 10752 (2002).
21. Z. H. Kim, H. A. Bechtel, R. N. Zare, *J. Am. Chem. Soc.* **123**, 12714 (2001).
22. M. P. Schmid, P. Maroni, R. D. Beck, T. R. Rizzo, *Rev. Sci. Instrum.*, **74**, 4110 (2003).
23. J. L. Duncan, M. M. Law, *Spectrochim. Acta A* **53**, 1445 (1997).
24. M. S. Child, L. Halonen, *Adv. Chem. Phys.* **57**, 1 (1984).
25. Of the two possible linear combinations of the $|20\rangle$ state, we excited the antisymmetric one, $|20\rangle^-$.
26. K. W. Busch, M. A. Busch, Eds., *Cavity Ringdown Spectroscopy*, vol. 720 of *ACS Symposium Series* (American Chemical Society, Washington, DC, 1999).
27. H. Yang, J. L. Whitten, *J. Chem. Phys.* **96** (1992).
28. G. J. Kroes, A. Gross, E. J. Baerends, M. Schieffler, D. A. McCormack, *Acc. Chem. Res.* **35**, 193 (2002).

29. Supported by Swiss National Science Foundation grants 200020-100058/1 and by the EPFL.

9 July 2003; accepted 19 August 2003

Identification of a Plant Nitric Oxide Synthase Gene Involved in Hormonal Signaling

Fang-Qing Guo, Mamoru Okamoto, Nigel M. Crawford*

Nitric oxide (NO) serves as a signal in plants. An *Arabidopsis* mutant (*Atnos1*) was identified that had impaired NO production, organ growth, and abscisic acid–induced stomatal movements. Expression of *AtNOS1* with a viral promoter in *Atnos1* mutant plants resulted in overproduction of NO. Purified AtNOS1 protein used the substrates arginine and nicotinamide adenine dinucleotide phosphate and was activated by Ca^{2+} and calmodulin-like mammalian endothelial nitric oxide synthase and neuronal nitric oxide synthase, yet it is a distinct enzyme with no sequence similarities to any mammalian isoform. Thus, *AtNOS1* encodes a distinct nitric oxide synthase that regulates growth and hormonal signaling in plants.

Nitric oxide (NO) functions as a signal and a cytotoxic agent in many physiological and immunological processes in animals (*1–3*) and is synthesized by nitric oxide synthase (NOS) (*2*, *4–6*). There are three known isoforms of NOS [neuronal (nNOS), inducible (iNOS), and endothelial (eNOS)], and each contains a heme-oxygenase and a flavin reductase domain. Related NOS genes have been described in many eukaryotic species from vertebrates to fungi (*6*, *7*). Bacteria also encode NOS proteins that are smaller, containing only the oxygenase domain, which is similar in sequence and biochemical activity to the mammalian NOS oxygenase (*8–10*).

In plants, NO serves as a signal in hormonal and defense responses (*3*, *7*, *11–14*). The source of NO synthesis in plants has

Section of Cell and Developmental Biology, Division of Biological Sciences, University of California at San Diego, La Jolla, CA 92093–0116, USA.

*To whom correspondence should be addressed. E-mail: ncrawford@ucsd.edu